

LAMINAR AIDING AND OPPOSING MIXED CONVECTION IN A VERTICAL CHANNEL WITH AN ASYMMETRIC DISCRETE HEATING AT ONE WALL

by

**Nassim LAOUCHE^a, Abdelkader KORICHI^a,
Catalin Viorel POPA^{b*}, and Guillaume POLIDORI^b**

^a Laboratory of Mechanics, Physics and Mathematical Modeling (LMP2M),
University of Medea, Medea, Algeria

^b GRESPI, University of Reims Champagne-Ardenne, Reims, France

Original scientific paper
<https://doi.org/10.2298/TSCI160105149L>

Detailed numerical simulations are carried out for aiding/opposing mixed convection in a rectangular channel with an asymmetric discrete heating. The governing equations were solved by the finite volume method using OpenFoam® open source code. Based on streamline patterns, temperature maps, velocity and thermal profiles, and Nusselt number evolution an extensive analysis on the effects of Richardson number in the range -5 to $+5$ for both opposed and aided buoyancy on the fluid flow and heat transfer characteristics is presented and discussed.

Key words: *mixed convection, aided/opposed buoyancy flow, discrete heat sources*

Introduction

Mixed convection from discrete heat sources is of interest in many practical applications, such as the cooling of electronics equipment, the heating of elements for positioning within events. The evacuation of the heat produced generates constraints on development, miniaturization, and compacting of systems operating at high level energy. Understanding the flow structure and heat transfer mechanisms in these equipments may significantly improve their design and then their cooling performance. The common ways used for the cooling in such situations include free, forced and mixed convection using air or liquid as the coolant. However, air cooling has been the most popular method due to its simplicity and low maintenance cost. When the systems are subjected to discrete wall heat sources, the heat transfer behavior is different from that encountered when the heat sources are continuous. Many experimental and numerical investigations on the characteristics of convective heat transfer in a parallel plate channel with discrete heating sources at wall are available in the literature. An extensive review of free and forced convection encountered in electronic cooling was conducted by Incropera *et al.* [1] and Peterson and Ortega [2]. Tewari and Jaluria [3] carried out an experimental investigation of mixed convection with discrete thermal sources on horizontal and vertical surfaces. They showed that the upstream heat source could affect the heat transfer performance of the downstream heat source if the separation distance is less than three strip widths. The magnitude of the effect was strongly dependent

* Corresponding author, e-mail: catalin.popa@univ-reims.fr

on the orientation of the heat sources. Hasnaoui *et al.* [4] investigated the pure natural and mixed convection at low Reynolds in a channel with periodic heat sources. In the case of mixed convection, they observed that the flow structure is considerably affected by the size of the heated element. Moreover, above the critical Reynolds number, the generated rolls were carried downstream with a time dependent velocity. Mixed convection in a horizontal channel with periodic temperature boundary condition has been investigated by Tangborn [5]. He showed that if the upper wall is insulated, the flow is stabilized and will not become unsteady unless the Reynolds number is raised to $Re = 100$. The critical Reynolds number will be lower if the fluid is unstably stratified. Choi and Ortega [6] studied the mixed convection in a parallel plate channel with one heat source under different orientations. Their results indicated that the overall Nusselt number of the source strongly depends on the inclination angle at high tilt ($>45^\circ$). However, the changes were negligible for inclination angle in the range $0-45^\circ$. Turkoglu and Yucel [7] examined the mixed convection heat transfer in a vertical channel with a single discrete heat source. They observed that the location of the heating element does not play a considerable role on the flow. Moreover, they noticed that the flow and heat transfer were controlled by Grashof number only at low Reynolds numbers (*e. g.* $Re < 50$). At higher values, Reynolds number plays an important role. In a 3-D channel with discrete heat sources attached to the bottom/top wall, Choi and Kim [8] observed that the flow structure and isotherms patterns exhibit a 3-D shape only when the source is attached to the top wall. Tsay [9] found that discrete heating can cause the heat transfer direction from fluid to the heated plate wall during the transient period in the unheated section as a result of axial wall conduction. This phenomenon increases with increasing the unheated step length. Wang and Jaluria [10] found that the discontinuous thermal boundary condition on the bottom makes the longitudinal rolls expand and shrink periodically, and helps in the generation of transverse rolls. In their study Wang and Jaluria [11] showed that the span wise arrangement of heat sources results in a lower global average temperature when compared to the stream-wise arrangement, for two heat sources distribution. Baskaya *et al.* [12] carried out an experimental investigation of mixed convection from an array of discrete heat sources at the bottom of a horizontal channel. They showed that the onset of the secondary flow induced by the buoyancy effect can enhance heat transfer. The onset of the secondary flow position depends on the Grashof to Reynolds numbers ratio. In the same subject Dogan *et al.* [13] pointed out that the onset of the secondary flow can affect the top surface only for small Reynolds numbers at low channel aspect ratios. Numerical investigation of mixed convection in a 3-D channel with discrete heating has been investigated by Cheng *et al.* [14]. Their results demonstrated that the Richardson number has more influence on the friction factor and on Nusselt number at high Reynolds numbers. The channel height also affects heat transfer and friction factor for a constant temperature boundary condition. Mathews *et al.* [15] studied numerically the effect of wall conduction on mixed convection in a vertical plate channel with discrete heating sources. They found that the maximum temperature of heat sources can be reduced significantly by increasing the thermal conductivity ratio (wall to fluid conductive) up to around 150. Rao [16] and Sawant and Rao [17] notified that the radiation can not be neglected for a large heating input, in particular in the cooling process by natural convection. Moreover, they showed that long narrow channels are unadvisable in comparison to relatively short broadly spaced channels. Da Silva and Gosselin [18] recommended non-uniform heat sources distribution to increase system conductance in forced convection regime. For large Grashof numbers, Martinez-Suastegui and Trevino [19] showed that the opposed buoyancy produces a vertical structure with one or several clockwise rotating vortices and strong transverse flow oscillations with increasing amplitudes in downstream positions. They reported that the Nusselt number first decreases and later increases with the Richardson number. Akdag

[20] observed a heat transfer enhancement up to 25% from discrete heat sources in channel using high amplitude pulsating flow compared to the steady-state flow. However, increasing the frequency causes negative effects on the heat transfer. Bairi *et al.* [21] showed that the convective results concerning the uniform heat flux conditions differ from those corresponding to uniform temperature ones on the heated bands on vertical walls under natural convection. Mixed convection in upward vertical channel flow with one wall spatially and periodically heated was studied by Dritselis *et al.* [22]. They showed that the spatially periodic wall temperature produces local re-circulating flow patterns. Recently an extensive review on the research status on convective heat transfer and channel flow cooling for heat sources was carried out by Bhowmik [23]. The review summarizes the published works in the two last decades that dealt with three convection modes over flush-mounted and protruded discrete heat sources.

From the previous literature review, it can be seen that the mixed convection heat transfers with multiple discrete heat sources under aiding and opposing buoyancy effect has received less attention. Thus, the aim of this paper is to conduct a detailed numerical of laminar aided/opposed mixed convection in a parallel plate channel with multiple discrete heat sources at one wall.

Physical configuration and mathematical formulation

The physical configuration and notations considered for the numerical analysis are illustrated in fig. 1. The system consists of a parallel-plate channel length, L , and width, H , with large aspect ratio. The right wall of the channel is equipped with four identical flush-mounted discrete heat sources with the same length and spacing H . The first heat source is located at a distance $L_e = 4H$ from the channel inlet while the last one is located at a distance $L_s = 10H$ from the outlet, so that the channel has a height of $21H$. In the present numerical investigation, the incompressible flow is assumed to be steady, laminar and 2-D in the range of used parameters. The buoyancy driven flow from the heated surface interacts with the laminar main flow to yield mixed convection conditions. Viscous dissipation is neglected and constant thermophysical

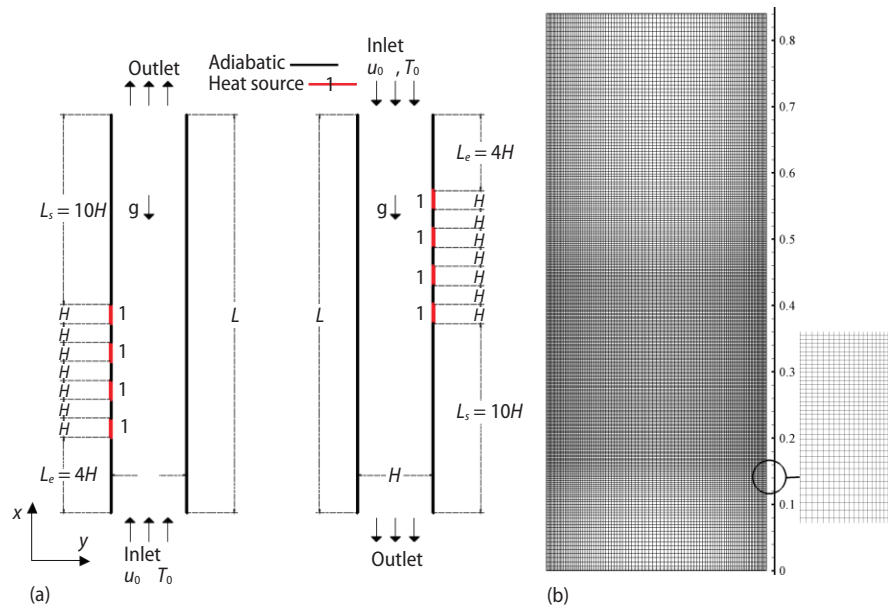


Figure 1. (a) Geometry of fluid domain, (b) mesh

properties of the medium are assumed, except for the density. Boussinesq approximation is used to estimate the thermal buoyancy term in the momentum equation.

Thus, the continuity, the x and y components of the Navier-Stokes equation and the energy equation in the dimensional form can be written:

$$\frac{\partial u}{\partial x} + \frac{\partial v}{\partial y} = 0 \quad (1)$$

$$\rho \left(u \frac{\partial u}{\partial x} + v \frac{\partial u}{\partial y} \right) = -\frac{\partial p}{\partial x} + \mu \left(\frac{\partial^2 u}{\partial x^2} + \frac{\partial^2 u}{\partial y^2} \right) \mp \rho_x g [1 - \beta(T - T_0)] \quad (2)$$

$$\rho \left(u \frac{\partial v}{\partial x} + v \frac{\partial v}{\partial y} \right) = -\frac{\partial p}{\partial y} + \mu \left(\frac{\partial^2 v}{\partial x^2} + \frac{\partial^2 v}{\partial y^2} \right) \quad (3)$$

$$u \frac{\partial T}{\partial x} + v \frac{\partial T}{\partial y} = \alpha \left(\frac{\partial^2 T}{\partial x^2} + \frac{\partial^2 T}{\partial y^2} \right) \quad (4a)$$

where α is thermal diffusivity, defined:

$$\alpha = \frac{k}{\rho c_p} \quad (4b)$$

The sign minus (−) in eq. (3) corresponds to the opposed buoyancy case while the sign plus (+) corresponds to the aided buoyancy case.

The boundary conditions used in this study are:

- at the channel inlet

$$u = u_0, \quad T = T_0 \quad (5a)$$

- at the outlet, an outflow boundary condition is given

$$\frac{\partial u}{\partial x} = 0, \quad \frac{\partial p}{\partial x} = 0, \quad \frac{\partial T}{\partial x} = 0 \quad (5b)$$

- at the wall: $u = v = 0$
 - surfaces of heat sources

$$T = T_0 \quad (5c)$$

- adiabatic condition at all other surfaces

$$\frac{\partial T}{\partial y} = 0 \quad (5d)$$

Numerical method

The governing transport equations associated with the boundary conditions were solved using the open source OpenFoam® code based on the finite volume formulation. The *buoyantBoussinesqSimpleFoam* solver is employed and it is based on the SIMPLE algorithm and uses the Boussinesq approximation for estimating the density in buoyancy term in the momentum equation. For the spatial discretization the central second order differencing scheme is used for both diffusive and convective terms. The iterative solution is continued until the resid-

uals for all computational cells become less than 10^{-6} for all dependent variables. The grid is chosen non-uniform and is highly concentrated close to the wall, particularly in the vicinity of the heated portions in order to capture high gradient velocity, pressure, and temperature. To ensure grid independence for the results, a series of tests for non-uniform grids were carried out. The nodes have been chosen equally spaced along the source, whereas an adequate expansion ratio characterizes the node distribution on the other edges of the domain.

The local Nusselt number evolution along the heated wall in the vicinity of the heated sources and obtained with four grid sizes tested (180×40 , 270×60 , 360×80 , and 450×100) at $Gr = 4 \cdot 10^4$ and $Ri = 1$ is shown in fig. 2. The maximum relative error in Nusselt number for 360×80 and 450×100 not exceeds 0.5%. Accordingly, the 360×80 grid is considered to be suitable for the present study.

The validation of the numerical simulation was attained by performing calculations for the case of mixed convection of a vertical channel and by comparing our results with those of Desrayaud and Lauriat [24] in their numerical study for a symmetric heating under the same conditions. Figures 3(a) and 3(b) compare the velocity and temperature profiles at different sections and it can be seen a good agreement between these two studies and the maximum relative error is less than 3%.

Results and discussion

The present investigation focuses on the flow structure and heat transfer characteristics in a vertical channel with four discrete heating sources at one wall. For the present study, the channel width was fixed to $H = 0.04$ m so that the channel is height 0.88 m. So, only to better understand the thermodynamically phenomena occurring in such mixed convection system, only the part of the channel close to the heated elements is represented.

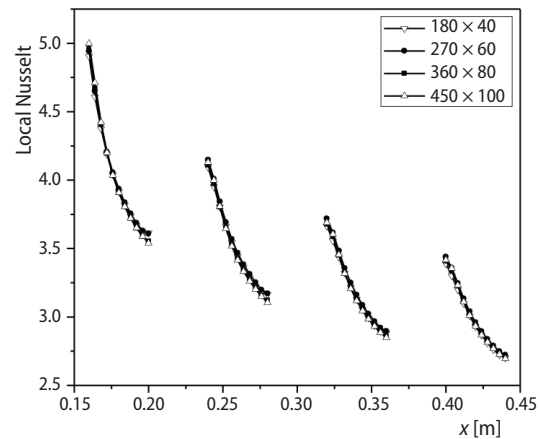


Figure 2. Nusselt number according to different mesh

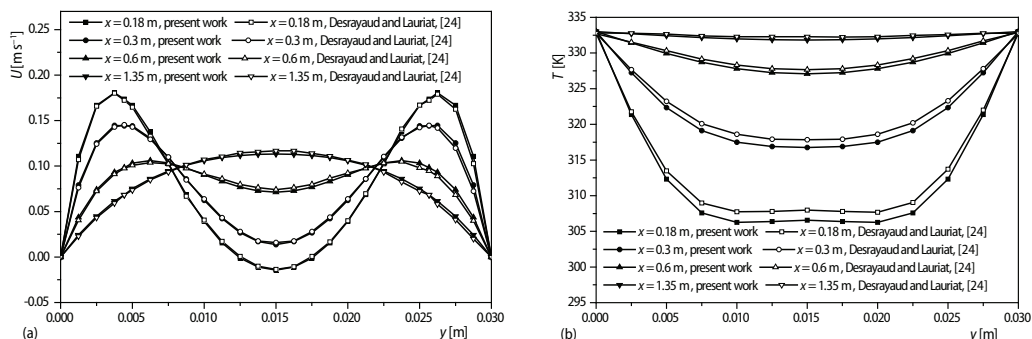


Figure 3. Validation of the present numerical simulation by comparison with the results of Desrayaud and Lauriat [24]; (a) velocity profiles, (b) temperature profiles

Table 1. Physical parameters used

Re	u_0 [ms ⁻¹]	T_∞ [K]	T_w [K]	ΔT [K]	Gr	Ri
200	0.0785	300	302.61	2.61	$2 \cdot 10^4$	0.5
200	0.0785	300	305.23	5.23	$4 \cdot 10^4$	1
200	0.0785	300	310.46	10.46	$8 \cdot 10^4$	2
200	0.0785	300	326.17	26.17	$2 \cdot 10^5$	5

Grashof number at a Reynolds number value equal to 200, using air ($Pr = 0.71$) as working fluid, tab. 1, leading to the ranges $0.5 \leq Ri \leq 5$ for aiding mixed convection and $-5 \leq Ri \leq -0.5$ for opposing mixed convection.

Assisted buoyancy flow ($Ri > 0$)

The contours of longitudinal (stream-wise) velocity component and stream-line patterns under buoyancy assisted condition are presented in figs. 4 and 5, respectively, for combinations of $Re = 200$ and Grashof number in the range $2 \cdot 10^4$ to $2 \cdot 10^5$, leading to $Ri = Gr/Re^2$ between 0.5 and 5. Whatever the Richardson number is the velocity magnitude exhibits a symmetrical behavior at the channel inlet as shown on fig. 4 where the heated wall is on the left. As the flow moves upstream in the channel, it accelerates near the heat sources as a result of buoyancy assisted effect resulting in a dissymmetry in the velocity contours. The dissymmetry becomes more pronounced increasing the Richardson number and is due to the acceleration of the fluid near the heated wall which is accompanied by a deceleration near the cold one to satisfy the mass balance. It can also be seen that the zone of high velocity moves downward increasing Richardson number at fixed $Re = 200$. Indeed, increasing Grashof number (or Ri at

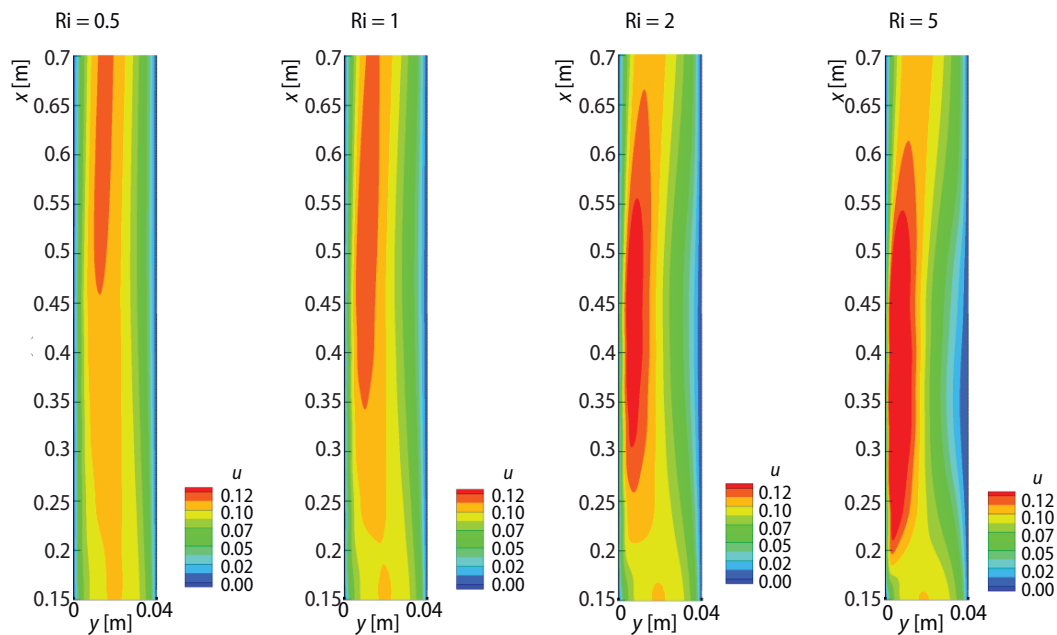


Figure 4. Contours of longitudinal velocity component under buoyancy assisted condition vs. Richardson number (for color image see journal web site)

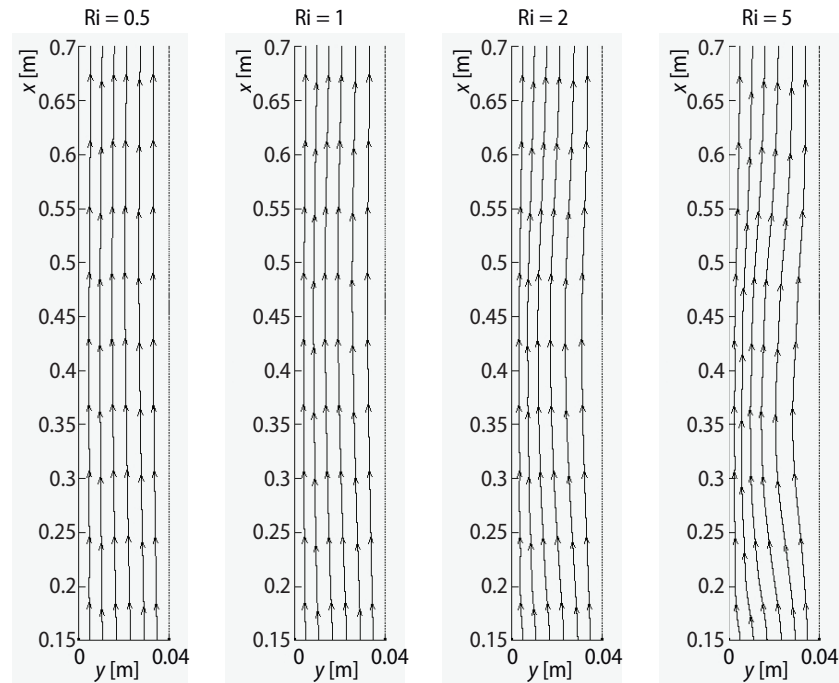


Figure 5. Streamlines under buoyancy assisted condition vs. Richardson number

fixed Re) produces a thinner boundary-layer in the vicinity of the heated wall, inducing a left shifting of the maximum velocity contours towards the wall containing the heated parts.

This asymmetry in the mass transfer is also appearing on the streamline patterns, fig. 5, where an inflexion of lines in closeness of the adiabatic wall is pronounced all the more as Richardson number increases. At low Grashof numbers, *e. g.* at low Richardson number, the streamlines are quasi-parallel and equispaced corresponding in what it can be expected in a forced convection regime flow. Looking more in detail the velocity and temperature profiles, figs. 6 and 7, at the exit of each heated zone for $Ri = 1$, leads to clearly confirm the acceleration

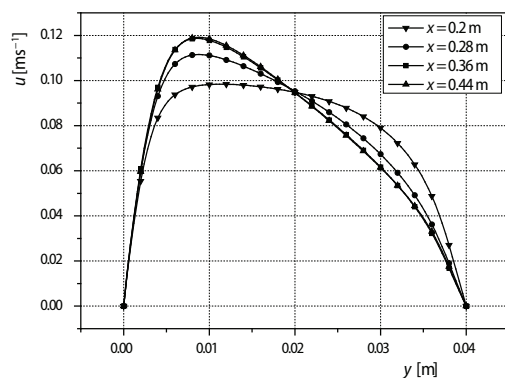


Figure 6. Stream-wise velocity profiles under buoyancy assisted condition at different sections for $Ri = 1$

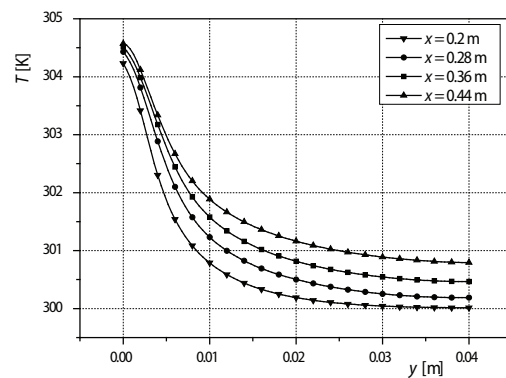


Figure 7. Temperature profiles under buoyancy assisted condition at different sections for $Ri = 1$

of the fluid as it rises in the channel. It seems clearly that the successive presence of the heating elements is going to break more and more the symmetry of the velocity profiles. The position of the maximum velocity remains confined in the vicinity of the heated wall and presents a gap of the order of 20% on its value at the exit of the first and last heated areas. From the thermal field, fig. 8, it can be seen that the isotherms contours are crowded in the immediate proximity of the heat sources, highlighting the highest temperature gradients. In the vicinity of the heating parts of the wall, the thermal boundary thickens more and more as it moves upward in the main flow direction. Beyond the last warmed zone, a decrease in the temperature gradient is observed leading to a thickening of the thermal boundary-layer. This can be confirmed by the temperature profiles at the end of the heat sources as shown in fig. 7. Increasing Richardson number, the isotherms extend in both axial and transversal directions to reach the opposite cold wall after only a distance of four times the length of the heat source. This is due to the fact that at high Richardson number the heat transfer by diffusion in the flow channel plays a non-negligible role as opposed to the forced convection where energy is transported away by the imposed incoming flow. Decreasing Richardson number, this distance increases until the isotherms become quasi-parallel materializing a trend to a forced convection regime.

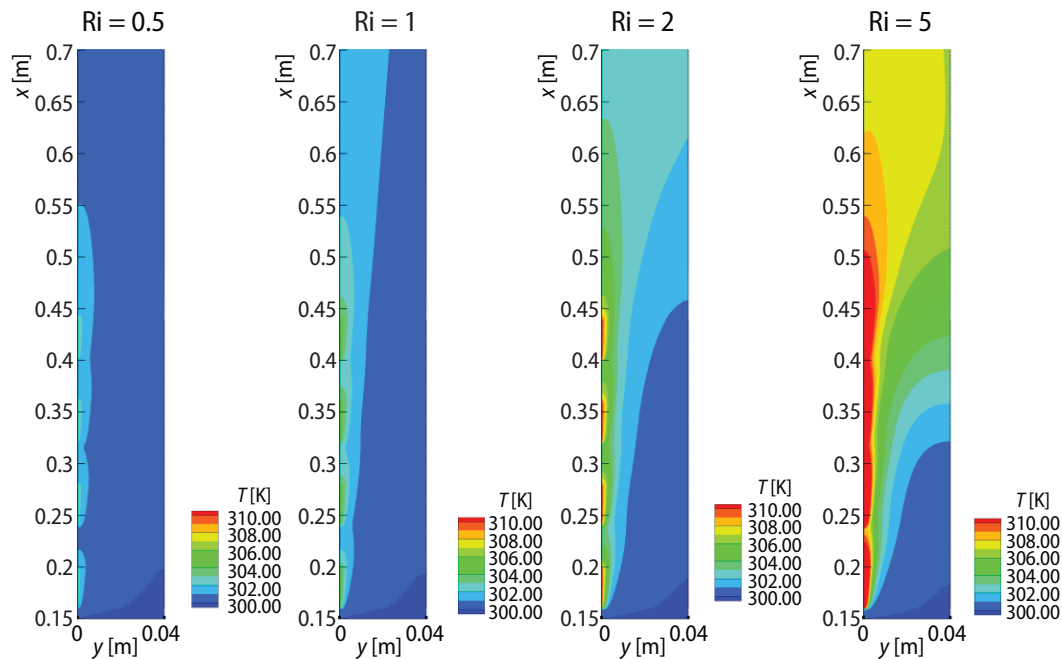


Figure 8. Thermal contours under buoyancy assisted condition vs. Richardson number
(for color image see journal web site)

Opposed buoyancy flow ($Ri < 0$)

In certain industrial applications and due to technical constraints, downward ventilation locally which opposes the ascending movement of the heat flow can locally occur. Thus, the thermal management of electronics devices for example under these conditions is crucial. In the case of opposed buoyancy flow, the buoyant forces generated by Archimedes principle as a result of decreasing of the density of fluid near the heated region oppose the inertial forces imposed at the inlet by a mechanical agent.

This phenomenon can lead locally to an accumulation of heat resulting in failure of the system. Depending on their relative magnitudes, the opposition of these forces can result in strong interactions between the two flows. It is recalled that for the opposing mixed convection problem, the main flow is now downward and the heated elements are located on the right wall. The velocity magnitude and streamlines under buoyancy opposed condition are shown in figs. 9 and 10, in the range $Ri = -0.5$ to -5 . It seems clearly in fig. 9 that contrary to the aiding mixed convection problem ($Ri > 0$), in the case of the opposed mixed convection, the longitudinal velocity outlines of stronger magnitude are pushed away in the neighborhood of the wall opposed to the heating one. A common point to these two mixed convection modes is that the more the Grashof number is high, the more this zone of higher velocities is situated close to the channel inlet, this phenomenon being however more pronounced in the case of the opposed mixed convection. Velocity outlines exhibit fluctuations with presence of negative velocities corresponding to the development of the natural convection boundary-layer on the heated wall, whose direction is opposed to that of the main flow. It can be seen in fig. 10 that when increasing Richardson number (in absolute value), the rolling-up of the ascendant boundary-layer leading to re-circulation cells appears in the vicinity of the heat sources. The re-circulation zones are the consequence of the interaction between the imposed downward flow and the upward buoyancy flow. The size and the magnitude of the re-circulation zones grow when the hot fluid moves up. Because the fluid passes from a heat source to another, the buoyancy force increase as a result of the augmentation of fluid temperature caused by the heat accumulation.

If for the two lowest zones of heating as well separation as attachment is present at wall, one can observe the coalescence of the two upper vortices forming a long eight shape zone of two co-rotating cells. At low Grashof number, *e. g.* at low Richardson number number, the effect of natural convection vanishes and the forced convection dominates, then the streamlines become quasi-parallel.

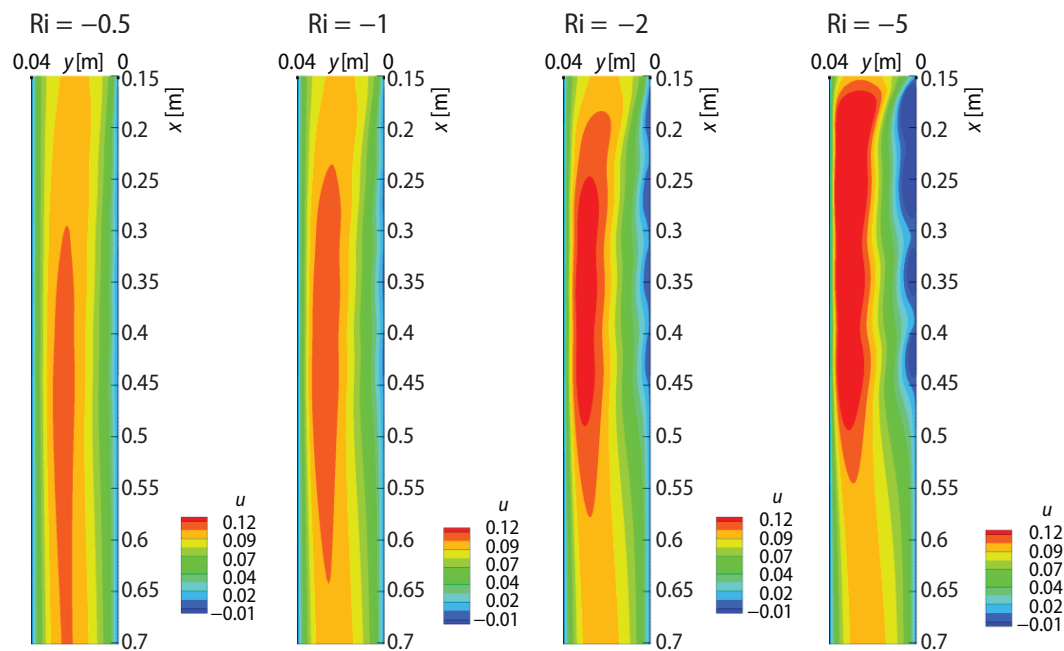


Figure 9. Contours of longitudinal velocity component under buoyancy opposed condition vs. Richardson number (for color image see journal web site)

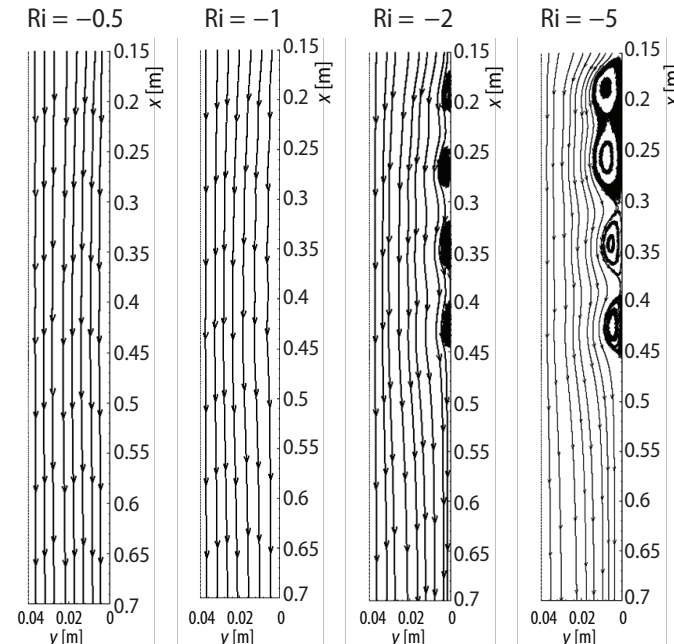


Figure 10. Streamlines under buoyancy opposed condition for Richardson number

tion. This phenomenon is more pronounced at high Richardson number, fig. 13. Away from the wall, the forced flow dominates and the hot fluid is carried away by the forced flow. Decreasing in Richardson number the phenomenon tends towards the pure forced convection situation. Profiles of the temperatures taken as example in fig. 12, traduce well the phenomenon of thickening of the thermal boundary-layer within the channel as we go away from the channel inlet.

Heat transfer characteristics

To understand the heat transfer characteristics in the channel flow, the Nusselt number evolution along the wall containing the heated sources is plotted for the aided buoyancy flow in

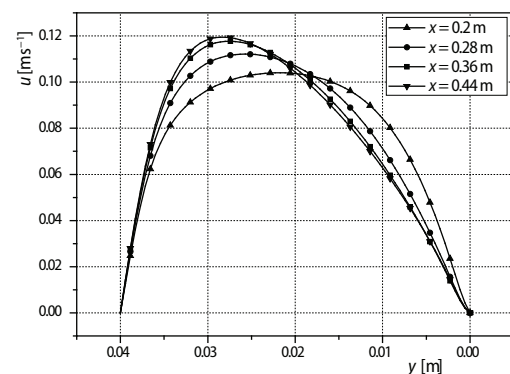


Figure 11. Stream-wise velocity profiles under buoyancy opposed condition at different sections for $Ri = -1$

In figs. 11 and 12 have been represented the velocity and temperature profiles for $Ri = -1$. If one looks at the profiles of velocity at various heights one can clearly see the phenomenon of the contraction of the stream-lines towards the wall opposed to the heating one as we go away from the inlet of the channel, fig. 11. For the thermal field, the isotherms contours imitate the flow interaction. In the re-circulation cells at the vicinity of the heat sources, where the fluid stays more time, the heat is mainly transferred by conduction (diffusion).

This mode is confirmed by the circular shape of the temperature contours with a slight expanding in the flow direction.

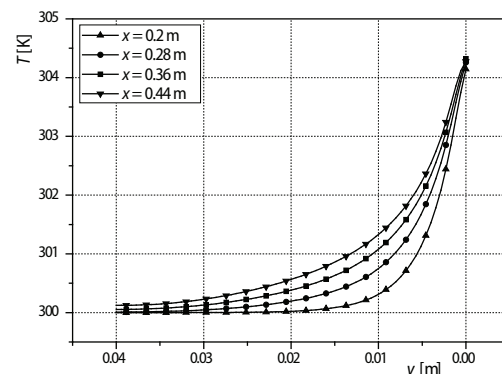


Figure 12. Temperature profiles under buoyancy opposed condition for $Ri = -1$

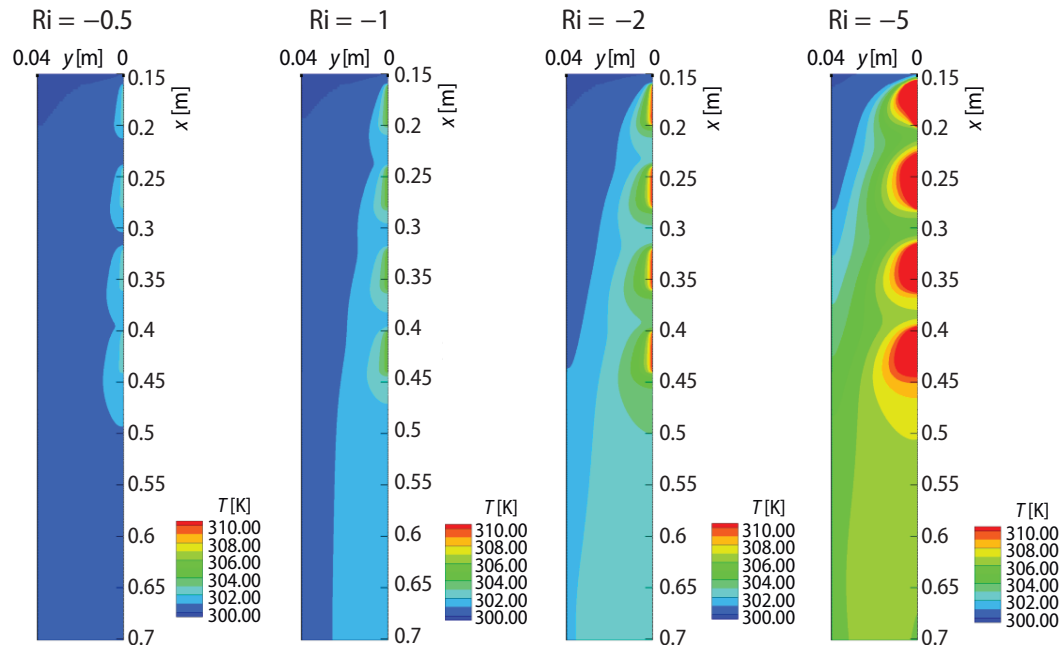


Figure 13. Thermal contours under buoyancy opposed condition vs. Richardson number
(for color image see journal web site)

fig. 14 in the range of Richardson number varying from 0.5 to 5. Whatever Richardson number is, the Nusselt number is high at the leading edge of each heating element and decreases along the heat source in the flow direction. So at the leading edge, there is no effect on heat transfer. As the fluid moves in the main stream-wise, its temperature raises leading in the decrease in the Nusselt number. One observes nevertheless a certain increase in Nusselt number when the fluid reaches the trailing edge of the heating zone, corresponding to the boundary where the fluid is in contact with the adiabatic colder wall facilitating heat transfer. It can be clearly observed that the values of the Nusselt number become higher with increasing the Richardson number. Indeed, as the fluid moves

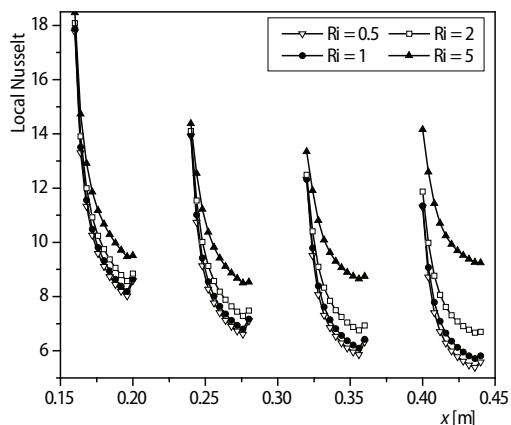


Figure 14. Nusselt number under assisted buoyancy condition vs. Richardson number

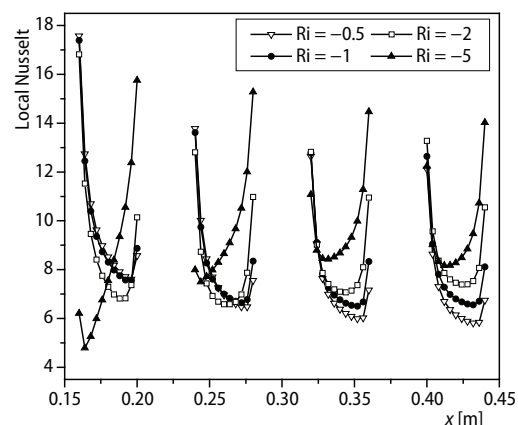


Figure 15. Nusselt number under opposed buoyancy condition vs. Richardson number

the buoyancy gains strength and accelerates the fluid, fig. 6, contributing to increase significantly the Richardson number. Globally, Nusselt number increases with increasing the Richardson number.

The Nusselt number evolution for the opposed buoyancy flow is plotted in fig. 15. For $Ri = -0.5$, $Ri = -1$, and $Ri = -2$, its behavior corresponds somewhat to that of the aiding mixed convection regime discussed early. For $Ri = -5$, the Nusselt number evolution exhibits a strange behavior. It decreases in the first portion of the heat source and then increases. The curves show a local minimum on the heat source segment in the vicinity of its leading edge. Unlike the aided mixed convection problem, the opposed situation highlights that this minimum tends to get closer to the leading edge of the warmed elements, and this especially as the Richardson number increases whatever the heat source location is. Globally, Nusselt number is minima for $Ri = -5$ close to the upper end of the first heat source, so that in practical application this can help to avoid placing a powerful heat source at the top of the channel.

Conclusions

In this study, a comprehensive analysis of aided/opposed mixed convection in a 2-D rectangular channel with discrete heat sources located on one wall has been carried out numerically. The governing equations were solved by the finite volume method using OpenFoam® open source code. The results revealed that the flow structure, temperature feature, and heat transfer were strongly dependent on the Richardson number for both aided and opposed mixed convection. It was found that in that case of aided buoyancy flow, a dissymmetry of the flow generated by addition of secondary flow produces thinner thermal boundary-layer leading to enhance heat transfer with increasing Richardson number, especially close to the channel outlet. In the case of opposed buoyancy flow, velocity and thermal maps are much more perturbed with the presence of rotating cells in close heated wall increasing Richardson number in absolute value. The consequence is a singular behavior in the heat transfer process for $Ri = -5$ with a low Nusselt number value close to the first heated element that the fluid encounters in its motion. This means that a particular attention has to be paid in the development of systems where evacuation of the produced heat needs an opposed mixed convection situation.

References

- [1] Incropera, F. P., et al., Convection Heat Transfer from Discrete Heat Sources in a Rectangular Channel, *Int. J. Heat Mass Transfer*, 29 (1986), 7, pp. 1051-1058
- [2] Peterson, G. P., Ortega, A., Thermal Control of Electronic Equipment and Devices, *Adv. Heat Transfer*, 20 (1990), Dec., pp. 181-314
- [3] Tewari, S., Jaluria, Y., Mixed Convection Heat Transfer from Thermal Sources Mounted on Horizontal and Vertical Surfaces, *ASME J. Heat Transfer*, 112 (1990), 4, pp. 975-987
- [4] Hasnaoui, M., et al., Mixed Convective Heat Transfer in a Horizontal Channel Heated Periodically from Below, *Numer. Heat Transfer A*, 20 (1991), 3, pp. 297-315
- [5] Tangborn, A., A Two-Dimensional Instability in a Mixed Convection Flow with Spatially Periodic Temperature Boundary Conditions, *Physics Fluids A*, 4 (1992), 7, pp. 1583-1586
- [6] Choi, C. Y., Ortega, A., Mixed Convection in an Inclined Channel with a Discrete Heat Source, *Int. J. Heat Mass Transfer*, 36 (1993), 12, pp. 3119-3134
- [7] Turkoglu, H., Yucel, N., Mixed Convection in Vertical Channels with a Discrete Heat Source, *Heat and Mass Transfer*, 30 (1995), 3, pp. 159-166
- [8] Choi, C. Y., Kim, S. J., Conjugate Mixed Convection in a Channel: Modified Five Percent Deviation Rule, *International Journal of Heat and Mass Transfer*, 39 (1996), 6, pp. 1223-1234
- [9] Tsay, Y. L., Transient Conjugated Mixed-Convective Heat Transfer in a Vertical Plate Channel with One Wall Heated Discretely, *Heat and Mass Transfer*, 35 (1999), 5, pp. 391-400
- [10] Wang, Q., Jaluria, Y., Instability and Heat Transfer in Mixed Convection Flow in a Horizontal Duct with Discrete Heat Sources, *Numerical Heat Transfer, Part A*, 42 (2002), 5, pp. 445-463

- [11] Wang, Q., Jaluria, Y., Three-Dimensional Conjugate Heat Transfer in a Horizontal Channel with Discrete Heating, *Journal of Heat Transfer*, 126 (2004), 4, pp. 642-647
- [12] Baskaya, S., *et al.*, Experimental Investigation of Mixed Convection from an Array of Discrete Heat Sources at the Bottom of a Horizontal Channel, *Heat Mass Transfer*, 42 (2005), 1, pp. 56-63
- [13] Dogan, A., *et al.*, Investigation of Mixed Convection Heat Transfer in a Horizontal Channel with Discrete Heat Sources at the Top and at the Bottom, *International Journal of Heat and Mass Transfer*, 49 (2006), 15-16, pp. 2652-2662
- [14] Cheng, Y. P., *et al.*, Numerical Analysis of Mixed Convection in Three-Dimensional Rectangular Channel with Flush-Mounted Heat Sources Based on Field Synergy Principle, *International Journal for Numerical Methods in Fluids*, 52 (2006), 9, pp. 987-1003
- [15] Mathews, R. N., *et al.*, Computation of Conjugate Heat Transfer in the Turbulent Mixed Convection Regime in a Vertical Channel with Multiple Heat Sources, *Heat Mass Transfer*, 43 (2007), Aug., pp. 1063-1074
- [16] Rao, C. G., Interaction of Surface Radiation with Conduction and Convection from a Vertical Channel with Multiple Discrete Heat Sources in the Left Wall, *Numerical Heat Transfer; Part A*, 52 (2007), 9, pp. 831-848
- [17] Sawant, S. M., Rao, C. G., Conjugate Mixed Convection with Surface Radiation from a Vertical Electronic Board with Multiple Discrete Heat Sources, *Heat Mass Transfer*, 44 (2008), Oct., pp. 1485-1495
- [18] Da Silva, A. K., Gosselin, L., Evolutionary Placement of Discrete Heaters in Forced Convection, *Numerical Heat Transfer A*, 54 (2008), 1, pp. 20-33
- [19] Martinez-Suastegui, L., Trevino C., Transient Laminar Opposing Mixed Convection in a Differentially and Asymmetrically Heated Vertical Channel of Finite Length, *International Journal of Heat and Mass Transfer*, 51 (2008), 25-26, pp. 5991-6005
- [20] Akdag, U., Numerical Investigation of Pulsating Flow around a Discrete Heater in a Channel, *International Communications in Heat and Mass Transfer*, 37 (2010), 7, pp. 881-889
- [21] Bairi, A., *et al.*, 2D Transient Natural Convection in Diode Cavities Containing an Electronic Equipment with Discrete Active Bands under Constant Heat Flux, *International Journal of Heat and Mass Transfer*, 55 (2012), 19-20, pp. 4970-4980
- [22] Dritselis, C. D., *et al.*, Buoyancy-Assisted Mixed Convection in a Vertical Channel with Spatially Periodic Wall Temperature, *International Journal of Thermal Sciences*, 65 (2013), Mar., pp. 28-38
- [23] Bhowmik, H., Review on Convection Heat Transfer in Channel Flow with Discrete Heater Arrays for Electronic Cooling, *International Journal of Engineering, Science and Technology*, 6 (2014), 2, pp. 31-44
- [24] Desrayaud, G., Lauriat, G., Flow Reversal of Laminar Mixed Convection in the Entry Region of Symmetrically Heated, Vertical Plate Channels, *International Journal of Thermal Sciences*, 48 (2009), 11, pp. 2036-2045